



## FTIR SPECTRUM AND XRD OF POSTBIOTICS-EXOPOLYSACCHARIDES ZINC OXIDE NANOPARTICLES

Krithika R\*<sup>1</sup>, Balasasirekha R<sup>2</sup>

<sup>1</sup>Research Scholar, Department of Food Science and Nutrition

<sup>2</sup>Avinashilingam Institute for Home Science and Higher Education for Women, Coimbatore, Tamil Nadu, India

\*Corresponding author: [krithikaravichandran1997@gmail.com](mailto:krithikaravichandran1997@gmail.com)

### ABSTRACT

The human body is occupied by millions of living microorganisms which all together, are called the human micro biota. Exopolysaccharides derived from lactic acid bacteria play a crucial role in improving the rheology, texture, mouth feel of fermented food formulations in food industry. The objective of the study was to characterise zinc oxide nanoparticles from postbiotics-exopolysaccharides and analyse the FTIR Spectrum and XRD of Postbiotics–Exopolysaccharides Zinc Oxide Nanoparticles. Postbiotics-exopolysaccharides was isolated from probiotic *Lactobacillus* culture medium using centrifugation method. Postbiotics-exopolysaccharides zinc oxide nanoparticles was synthesised by direct precipitation method using zinc sulphate and sodium hydroxide as precursor and characterisation was done using Fourier Transformed Infrared Spectroscopy (FTIR) and X-Ray Diffraction analysis. Results revealed that 46% of carbohydrate and 10% of protein content confirmed the presence of exopolysaccharides and in particular postbiotics-exopolysaccharides. The peak at 346.3 nm by Ultraviolet-Visible spectroscopy confirmed the presence of nanoparticles. The functional groups of postbiotics-exopolysaccharides zinc nanoparticles was recorded by Fourier Transform Infrared Spectroscopy using SHIMADZU Miracle spectrophotometer (FTIR 820IPC) KBr techniques. The scanning electron micrograph confirmed that postbiotics-exopolysaccharides zinc oxide nanoparticles had a rough, rigid and compact surface structure. The sharp narrow peak obtained in the graph by X-ray Diffraction Analysis confirmed the crystalline structure. The crystalline size of the postbiotics-exopolysaccharides zinc oxide nanoparticles as calculated by Debye-Scherrer equation  $D = K \lambda / \beta (\cos \theta)$  with highest peak value 34.01 confirmed the crystalline size to be 33.31 nm.

**Keywords:** Postbiotics, Exopolysaccharides, Zinc oxide nanoparticles, Fourier Transformed Infrared Spectroscopy (FTIR), X-Ray Diffraction Analysis (XRD).

### 1. INTRODUCTION

Postbiotics are defined as “any factor resulting from the metabolic activity of a probiotic or any released molecule capable of conferring beneficial effects to the host in a direct or indirect way”. It is derived each extracellular and intracellular. Exopolysaccharides are one of the most important secondary metabolites which are secreted externally to the cell surface. Exopolysaccharides have positive effect on health such as antitumor effects, antiulcer, antioxidant activities, immune stimulatory activity and also lowers blood cholesterol. Exopolysaccharides determined from lactic corrosive microscopic organisms. Zinc nanoparticles have excellent property of anticancer and antibacterial and it is also low in cost and less in toxicity. Zinc oxide nanoparticles, synthesized using microbial exopolysaccharides, are used as antibacterial food packaging coating to improve the shelf

life of the food products.

Postbiotics refers to soluble factors, products or metabolic products i.e. Metabolites secreted by live bacteria or released after bacterial lysis i.e. cell free supernatants such as polysaccharides, cell surface proteins and organic acids. It is derived both extracellular and intracellular [1]. Exopolysaccharides are one of the most important secondary metabolites which are secreted externally to the cell surface. Exopolysaccharides have positive effect on health such as antitumor effects, antiulcer, antioxidant activities, immune-stimulatory activity and also lowers blood cholesterol. The exopolysaccharides is an important feature of some strains of dairy lactic acid bacteria [2]. Lactic Acid Bacteria especially *Lactobacillus fermentum* has double functional properties antimicrobial activity against intestinal pathogens and high Total Antioxidative Activity

(TAA) and Total Anti-oxidative Status (TAS) of intact cells. It also plays an important role in improving Low Density Lipid (LDL) particles, i.e. the anti-atherogenic effect [3].

Zinc is a nutritional supplement and food additive. Zinc oxide nanoparticles affect the growth of many bacteria like *Staphylococcus*, *Streptococcus* and *E.coli*. Currently, there are widespread applications of zinc oxide nanoparticles in medicine because of their anti-bacterial effect. The food industry uses zinc oxide as a source of zinc, which is an essential micronutrient. Zinc nanoparticles have excellent property as anticancer and antibacterial and it is also low in cost and less in toxicity [4]. Zinc oxide is currently listed as a Generally Recognized As Safe (GRAS) material by the Food and Drug Administration. Thus, zinc oxide in Nano scale has shown antimicrobial properties and potential applications in food preservation. The main objective of this study was to synthesize and characterize the postbiotics-exopolysaccharides zinc oxide nanoparticles and to develop antimicrobial food packaging coating material for extending the shelf life of the food products [5].

## 2. MATERIALS AND METHODS

### 2.1. Isolation of probiotic *Lactobacillus*

Probiotic *Lactobacillus* species was isolated from Cow's raw milk using MRS broth (DeMan, Rogosa and Sharpe). The raw milk was diluted using distilled water in different ratios  $10^{-1}$   $\mu$ L,  $10^{-2}$   $\mu$ L,  $10^{-3}$   $\mu$ L and  $10^{-4}$   $\mu$ L.  $10^{-2}$   $\mu$ L serial dilution was used and poured in the spread plate method. This method helps to identify the species present in the milk and was identified as *Lactobacillus fermentum*.

### 2.2. Isolation of postbiotics-exopolysaccharides

Postbiotics-exopolysaccharides from probiotic *Lactobacillus* culture medium was isolated using centrifugation method. The MRS broth containing probiotic *Lactobacillus fermentum* cells were centrifuged at 8000 rpm for 20 min. The supernatant was collected to remove the *Lactobacillus fermentum* cells. The supernatant containing exopolysaccharides were precipitated using 3 volumes of chilled 95% ethanol and incubated at 44°C for 24 hours and allowed to stand overnight at 4°C in a refrigerator. The precipitate formed was again centrifuged at 8000 rpm for 20 min to obtain cell free solution. The precipitate was dissolved in 10% TCA (Tri Chloro Acetic acid) and stored at 4°C for 1 hour. The exopolysaccharides was then dissolved and dialyzed in distilled water for 4 days at 4°C. The cell free extract precipitate filled bag was kept

inside the beaker containing distilled water. The water acts as a buffer solution and helps to separate small molecules and protein present in the dialysed bag.

### 2.3. Test for protein and carbohydrate

Confirmation test for postbiotics-exopolysaccharides was done using protein and carbohydrate estimation of the dialysed postbiotics exopolysaccharides using standard procedures. To estimate protein, 0.5 ml of the dialysed postbiotics-exopolysaccharides was added with 2.5 ml of the solution C, mixed well and incubated for 10 min at room temperature. After incubation 0.2 ml of Folin's phenol reagent was added and the blue colour developed was measured at 660 nm in spectrophotometer. To estimate carbohydrate, 0.5 ml of the dialysed postbiotics-exopolysaccharides was added with 2.5 ml of the Anthrone reagent and incubated in a water bath at 100°C for 10-15 min measured at 620 nm in spectrophotometer.

### 2.4. Synthesis of postbiotics-exopolysaccharides zinc oxide nanoparticles

Postbiotics-exopolysaccharides zinc oxide nanoparticles was synthesised by direct precipitation method using zinc sulphate and sodium hydroxide as precursor. To 20 ml of 0.5 M zinc sulphate solution NaOH solution was added and mixed continuously using magnetic stirrer. To the mixture, one ml of dialysed postbiotics-exopolysaccharides was added into the beaker by stirring continuously, postbiotics-exopolysaccharides precipitated after 2-3 hours.

### 2.5. Characterization of postbiotics-exopolysaccharides zinc oxide nanoparticles

Chemical structure of postbiotics-exopolysaccharides zinc oxide nanoparticles was characterized using Fourier Transform Infrared (FTIR) Spectroscopy. Fourier Transform Infrared (FTIR) Spectroscopy shows the intensity of the peak absorbance of the functional groups of postbiotics-exopolysaccharides zinc oxide nanoparticles and the nature, size, composition and degree of crystallinity of the Postbiotics-exopolysaccharides zinc oxide nanoparticles was determined by using X-ray Powder Diffraction analytical technique.

#### 2.5.1. Fourier Transformed Infrared Spectroscopy (FTIR)

The functional groups of postbiotics-exopolysaccharides zinc nanoparticles were recorded using Fourier Transform Infrared Spectroscopy using SHIMADZU

Miracle spectrophotometer (FTIR 820IPC) KBr techniques. Infrared spectra were recorded between ranges 4000 to 400  $\text{cm}^{-1}$ . The unit of measurement of FTIR is  $\text{cm}^{-1}$ .

### 2.5.2. X-Ray Diffraction (XRD) Analysis

XRD studies were performed on the BrukerD8 advanced model XRD with running condition of 30 mA, 45 kV. X-rays were calculated using Bragg's law ( $n\lambda = 2d \sin \theta$ ). XRD pattern of synthesized postbiotics-exopolysaccharides zinc oxide nanoparticles is clearly indicated by sharp/narrow peaks confirming the crystalline structure. The unit of measurement of XRD is Angstroms.

## 3. RESULTS AND DISCUSSION

### 3.1. Postbiotics Polysaccharides

Protein content of dialysed postbiotics- exopolysaccharides was found to be 10%. Protein estimation helps to analyse the quality of dialysed postbiotics-

exopolysaccharides. The carbohydrate content of dialysed postbiotics - exopolysaccharides is 46%. It is also evident that the polysaccharides are having more amount of carbohydrate (46%) and less protein (10%) confirming the presence of polysaccharides.

### 3.2. Fourier Transformed Infrared Spectroscopy (FTIR) Analysis

The functional groups present in postbiotics-exopolysaccharides zinc oxide nanoparticles are characterized using FTIR.

Fig. 1 and Table 1 shows the peak absorbance values of postbiotics-exopolysaccharides zinc oxide nanoparticles.

The functional groups of postbiotics-exopolysaccharides zinc oxide nanoparticles were recorded using Fourier Transform Infrared Spectroscopy using SHIMADZU Miracle spectrophotometer (FTIR 820IPC) KBr techniques. Infrared spectra were recorded between ranges 4000 to 400 $\text{cm}^{-1}$ .

**Table 1: Peak absorbance values of postbiotics - exopolysaccharides zinc oxide nanoparticles using FTIR spectroscopy**

Functional Group	Frequency Standard ( $\text{cm}^{-1}$ )	Frequency Obtained( $\text{cm}^{-1}$ )	Intensity
Water OH stretch	3700-3100	3695.61 $\text{cm}^{-1}$	Strong
Alcohol OH stretch	3600-3200	3595.31 $\text{cm}^{-1}$	Strong
Carboxylic acid OH stretch	3600-2500	3595.31 $\text{cm}^{-1}$	Strong
N-H stretch	3500-3350	3471.87 $\text{cm}^{-1}$	Strong
$\equiv\text{C-H}$ stretch	$\sim 3300$	3302.13 $\text{cm}^{-1}$	Strong
$=\text{C-H}$ stretch	3100-3000	3194.12 $\text{cm}^{-1}$	Weak
-C-H stretch	2950-2840	2978.09 $\text{cm}^{-1}$	Weak
-C-H aldehydic	2900-2800	2885.51 $\text{cm}^{-1}$	Strong
$\text{C}\equiv\text{N}$ stretch	$\sim 2250$	2337.72 $\text{cm}^{-1}$	Strong
$\text{C}\equiv\text{C}$ stretch	2260-2100	2337.72 $\text{cm}^{-1}$	Strong
$\text{C}=\text{O}$ aldehyde	1740-1720	1643.35 $\text{cm}^{-1}$	Strong
$\text{C}=\text{O}$ anhydride	1840-1800, 1780-1740	1643.35 $\text{cm}^{-1}$	Weak, strong
$\text{C}=\text{O}$ ester	1750-1720	1643.35 $\text{cm}^{-1}$	Strong
$\text{C}=\text{O}$ ketone	1745-1715	1643.35 $\text{cm}^{-1}$	Strong
$\text{C}=\text{O}$ amide	1700-1500	1643.35 $\text{cm}^{-1}$	Strong
$\text{C}=\text{C}$ alkene	1680-1600	1643.35 $\text{cm}^{-1}$	Weak
$\text{C}=\text{C}$ aromatic	1600-1400	1566.20 $\text{cm}^{-1}$	Weak
C-O-C stretch	1250-1050 several	1064.71 $\text{cm}^{-1}$	Strong
C-OH stretch	1200-1020	1064.71 $\text{cm}^{-1}$	Strong
$\text{NO}_2$ stretch	1600-1500 , 1400-1300	1566.20 $\text{cm}^{-1}$	Strong
C-F	1400-1000	1064.35 $\text{cm}^{-1}$ 1265.30 $\text{cm}^{-1}$	Strong
C-Cl	800-600	763.81 $\text{cm}^{-1}$	Strong
C-Br	750-500	763.81 $\text{cm}^{-1}$ , 671.23 $\text{cm}^{-1}$	Strong
C-I	$\sim 500$	416.62 $\text{cm}^{-1}$ , 501.49 $\text{cm}^{-1}$	Strong

Strong - indicates low transmittance; Weak - indicates high transmittance; Variable - indicates varying transmittance

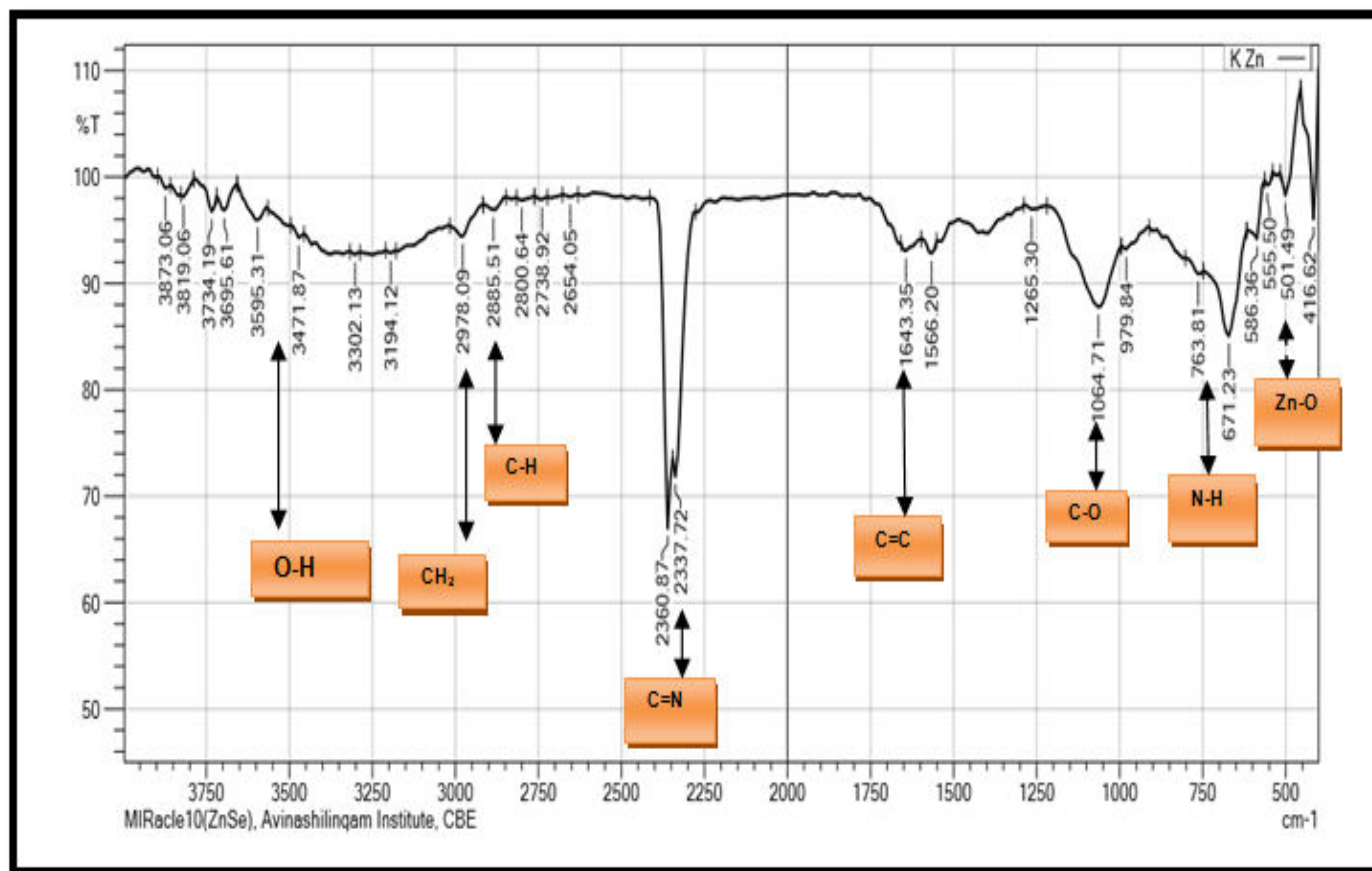


**Fig. 1: FTIR Spectra of Postbiotics-Exopolysaccharides Zinc Oxide Nanoparticles**

The peak frequency observed at  $3695.61\text{cm}^{-1}$  corresponds to water OH stretching and is between the standard frequencies ( $3700\text{--}3100\text{ cm}^{-1}$ ). The peak frequency observed at  $3595.31\text{ cm}^{-1}$  corresponds to the alcohol OH stretching and the standard frequency is  $3600\text{--}3200\text{ cm}^{-1}$ . The peak frequency observed at  $3595.31\text{ cm}^{-1}$  corresponds to the carboxylic acid OH stretching and is between  $3600\text{--}2500\text{ cm}^{-1}$ , the standard frequency. The peak frequency observed at  $3471.87\text{ cm}^{-1}$  corresponds to the N-H stretching and the corresponding standard frequency lies between  $3500\text{--}3350\text{ cm}^{-1}$ . The peak frequency observed at  $3302.13\text{ cm}^{-1}$  corresponds to the  $\equiv\text{C-H}$  stretching and is well within the standard frequency ( $\sim 3300\text{ cm}^{-1}$ ).

The peak frequency observed at  $3194.12\text{ cm}^{-1}$  corresponds to the  $=\text{C-H}$  stretching and lies between the standard frequency of  $3100\text{--}3000\text{ cm}^{-1}$ . The peak frequency observed at  $2978.09\text{ cm}^{-1}$  corresponds to -C-H stretching ( $2950\text{--}2840\text{ cm}^{-1}$ ). The peak frequency observed at  $2885.51\text{ cm}^{-1}$  corresponds to -C-H aldehydic ( $2900\text{--}2800\text{ cm}^{-1}$ ). The peak frequency observed at  $2337.72\text{ cm}^{-1}$  corresponds to the  $\text{C}\equiv\text{N}$

stretching and its standard frequency is  $\sim 2250\text{ cm}^{-1}$ . The peak frequency observed at  $2337.72\text{ cm}^{-1}$  corresponds to the  $\text{C}\equiv\text{C}$  stretching (standard frequency  $2260\text{--}2100\text{ cm}^{-1}$ ). The peak frequency observed at  $1643.35\text{ cm}^{-1}$  corresponds to the  $\text{C}=\text{O}$  aldehyde and the standard frequency ranges between  $1740\text{--}1720\text{ cm}^{-1}$ . The peak frequency observed  $1643.35\text{ cm}^{-1}$  corresponds to  $\text{C}=\text{O}$  anhydride ( $1840\text{--}1800\text{ cm}^{-1}$ ,  $1780\text{--}1740\text{ cm}^{-1}$ ). The peak frequency observed at  $1643.35\text{ cm}^{-1}$  corresponds to the  $\text{C}=\text{O}$  ester with a standard frequency lying between  $1750\text{--}1720\text{ cm}^{-1}$ . The peak frequency observed at  $1643.35\text{ cm}^{-1}$  corresponds to the  $\text{C}=\text{O}$  ketone with a standard frequency of  $1745\text{--}1715\text{ cm}^{-1}$ . The peak frequency observed at  $1643.35\text{ cm}^{-1}$  corresponds to  $\text{C}=\text{O}$  amide ( $1700\text{--}1500\text{ cm}^{-1}$ ).

The peak frequency observed at  $1643.35\text{ cm}^{-1}$  corresponds to  $\text{C}=\text{C}$  alkene which has a standard frequency of  $1680\text{--}1600\text{ cm}^{-1}$ . The peak frequency observed at  $1566.20\text{ cm}^{-1}$  corresponds to the  $\text{C}=\text{C}$  aromatic and it has a standard frequency of  $1600\text{--}1400\text{ cm}^{-1}$ . The peak frequency observed at  $1064.71\text{ cm}^{-1}$  corresponds to the C-O-C stretch and lies between the

standard ranges of 1250-1050  $\text{cm}^{-1}$ . The peak frequency observed at 1064.71  $\text{cm}^{-1}$  corresponds to the C-OH stretching (1200-1020 $\text{cm}^{-1}$ ).

The peak frequency observed at 1566.20  $\text{cm}^{-1}$  corresponds to  $\text{NO}_2$  stretching and it lies between the standard ranges of 1600-1500  $\text{cm}^{-1}$ . The peak frequency observed at 1064.35  $\text{cm}^{-1}$  and 1265.30  $\text{cm}^{-1}$  corresponds to the C-F bond which is well within the standard range of 1400-1000  $\text{cm}^{-1}$ . The peak frequency observed at 763.81  $\text{cm}^{-1}$  corresponds to the C-Cl bond and is between the standard range 800-600  $\text{cm}^{-1}$ . The peak frequency observed at 763.81 $\text{cm}^{-1}$  and 671.23  $\text{cm}^{-1}$  corresponds to the C-Br bond between the standard ranges between 750-500  $\text{cm}^{-1}$ . The peak frequency observed at 416.62 $\text{cm}^{-1}$  and 501.49  $\text{cm}^{-1}$  corresponds to C-I bond with a standard range of  $\sim 500 \text{ cm}^{-1}$ .

The values obtained in the present study are in line with the studies by [6] who reported the peak values were observed at 416.62 $\text{cm}^{-1}$ , 501.49 $\text{cm}^{-1}$ , 555.50 $\text{cm}^{-1}$  and 586.36 $\text{cm}^{-1}$  corresponds to Zn-O stretching between 600-450 $\text{cm}^{-1}$ . The metal oxides generally give absorption peaks in the regions between 600 and 400 $\text{cm}^{-1}$ . The peak values observed at 671.23 $\text{cm}^{-1}$  and 763.81 $\text{cm}^{-1}$  corresponds to N-H of primary amines between 910-665 $\text{cm}^{-1}$ . The peak values absorbed at 1064.71 corresponds to carbohydrate band (C-O) between 1000 $\text{cm}^{-1}$ -1200 $\text{cm}^{-1}$ . The peak values between 1000 and 1125 $\text{cm}^{-1}$  shows the presence of uronic acid. The wave number region from 1200 $\text{cm}^{-1}$  to 800 $\text{cm}^{-1}$  is the fingerprint region to characterize different poly-

saccharides and was observed at 1064.71 $\text{cm}^{-1}$ . The stretching peak was observed at 1566.20 $\text{cm}^{-1}$  and 1643.35 $\text{cm}^{-1}$  which corresponds to the ring stretching of galactose and mannose (1662 $\text{cm}^{-1}$ -1593 $\text{cm}^{-1}$ ). C-H stretching of methyl group is at 2885.51 $\text{cm}^{-1}$  and amide group at peak 1643.35 $\text{cm}^{-1}$ . The peak 2978.09  $\text{cm}^{-1}$  was attributed to the symmetrical stretching vibration of aliphatic ( $\text{CH}_2$ ) group which revealed the presence of sugar content. The peak value 3302.13 $\text{cm}^{-1}$  revealed the presence of (O-H) group. The peak value 2885.51 $\text{cm}^{-1}$  indicates the presence of (C-H) group as inferred by [7]. The peak value 1643.35 $\text{cm}^{-1}$  corresponded to the C=C group. The peak value 2978.09 $\text{cm}^{-1}$  indicates the presence of  $-\text{CH}_2$  group. The peak value 1064.71 $\text{cm}^{-1}$  revealed the presence of C-O group. The peak values 3320.13 $\text{cm}^{-1}$ , 3471.87 $\text{cm}^{-1}$  and 3595.31  $\text{cm}^{-1}$  corresponds to Hydroxyl group (OH) of polysaccharides between (3600 $\text{cm}^{-1}$ -3200 $\text{cm}^{-1}$ ).

### 3.3. X-Ray Diffraction Analysis

X-ray diffraction (XRD) is used for determining various materials and allows measurement spacing between layers of atoms or atomic planes and determination of crystal structure of an unknown material. In XRD graph, broad peak indicates the amorphous structure of postbiotics - exopolysaccharides zinc oxide nanoparticles. Sharp/narrow peaks indicate the crystalline nature of postbiotics - exopolysaccharides zinc oxide nanoparticles.

**Table 2: X-ray diffraction of postbiotics-exopolysaccharides zinc oxide nanoparticles**

Peak Position ( $2\theta$ )	Height (cms)	FWHM Left ( $2\theta$ )	d-spacing ( $\text{\AA}$ )	Relative intensity (%)
28.28	128.32	0.1004	3.15519	5.35
29.99	255.87	0.1338	2.97940	10.67
31.34	370.86	0.1338	2.85405	15.46
31.94	114.80	0.2007	2.80197	4.79
32.55	161.57	0.1673	2.75034	6.73
34.01	2399.01	0.0502	2.63605	100.00
34.89	138.39	0.2676	2.57110	5.77
36.05	68.84	0.3346	2.49112	2.87
38.95	87.19	0.1673	2.31196	3.63
44.26	619.81	0.0836	2.04646	25.84
48.9	91.23	0.2676	1.86212	3.80
50.3	88.19	0.2007	1.81360	3.68
56.75	52.40	0.3264	1.62066	2.18
62.42	304.38	0.0612	1.48649	12.69

FWHM- Full Width at Half Maximum; d-spacing - inter atomic spacing; ( $\text{\AA}$ )- Angstrom

XRD studies were performed on the BrukerD8 advanced model XRD with running condition of 30 mA, 45 kV. X-rays were calculated using Bragg's law ( $n\lambda = 2d \sin\theta$ ). XRD pattern of synthesized postbiotics-exopoly-saccharides zinc oxide nanoparticles is clearly indicated by sharp/narrow peaks confirming the crystalline structure and is presented in Fig. 2.

Table 2 shows that XRD sharp diffraction peaks and their corresponding heights, Full Width at Half Maximum (FWHM), d-spacings and relative intensity.

The sharp diffraction peaks for  $2\theta$  positions are 28.28, 29.99, 31.34, 31.94, 32.55, 34.01, 34.89, 36.05, 38.95, 44.26, 48.9, 50.3, 56.75 and 62.42 degrees. The sharp diffraction peaks at position 28.28, 29.99,

34.89, 48.9 and 50.3 shows that partial crystalline nature of postbiotics-exopolysaccharides zinc oxide nanoparticles. Similar results were closed agreement with the study [8] with peak position of 28.67, 34.75, 38.24 and 44.32. The peak 38.95 and 44.26 shows the crystalline nature of the zinc oxide nanoparticles. The peaks 31.34, 31.94, 34.01, 36.05, 56.75 and 62.42 showing the synthesized zinc oxide nanoparticles were identical to hexagonal phase of zinc oxide. These results are in coincidence with the study [9] with peak position of 31.77, 34.44, 36.28, 56.52 and 62.88. The peaks obtained using XRD analysis were well in agreement with the research articles and also results was well matched with the JCPDS software.

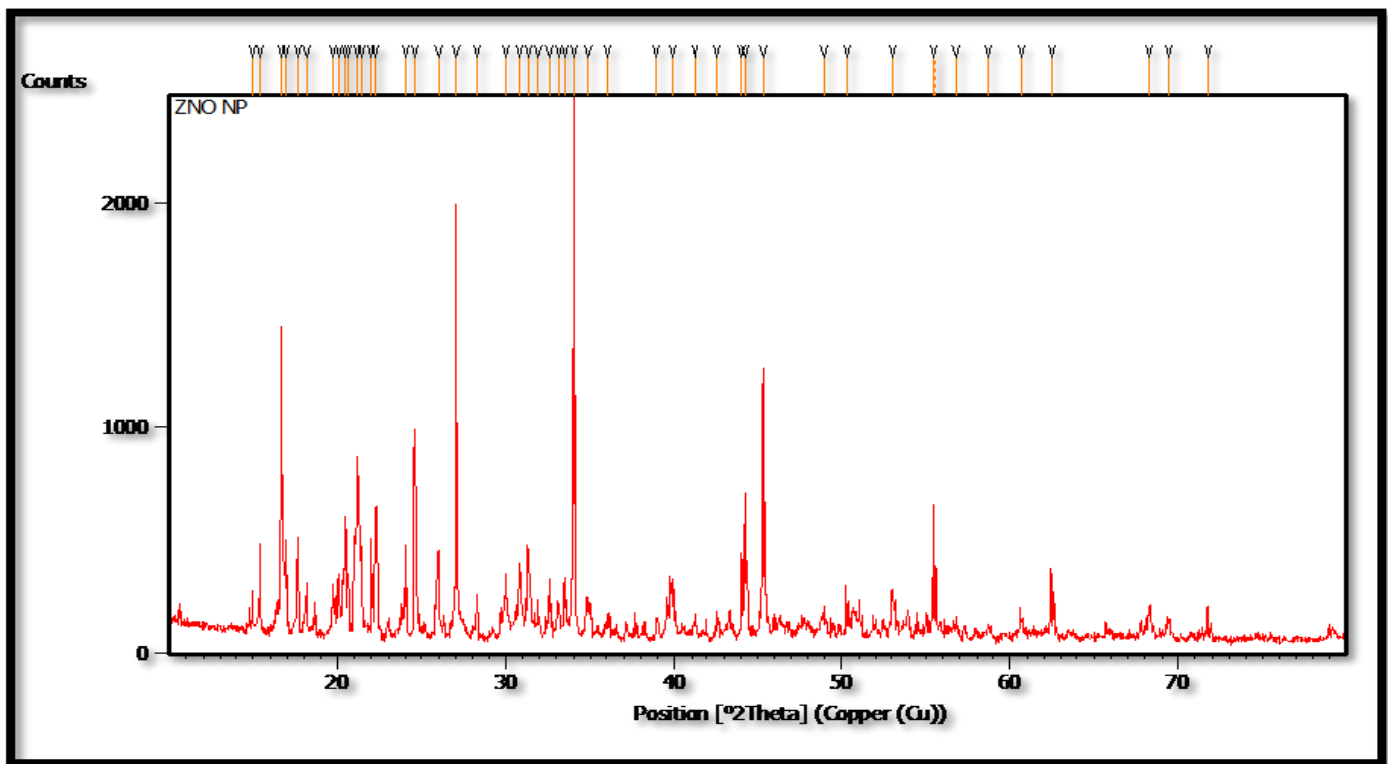


Fig. 2: X-Ray diffraction peaks of postbiotics-exopolysaccharides zinc oxide nanoparticles

The average size of zinc nanoparticles was calculated from the highest intense peak using the Debye-Scherer equation

$$D = K\lambda / \beta(\cos\theta)$$

Where  $\lambda$  is the wavelength of the X-rays used for diffraction and is equal to (1.540560 Å),  $\beta$  is full width at half maximum (FWHM) of the peak,  $\theta$  is the highest peak position and K is the shape factor and its value is equal to 0.9. The highest peak is at 34.01  $2\theta$  peak position which corresponds to 2399.01 peak height.

Hence,  $\theta=34.01$  and  $D = 33.31$  nm i.e. the average size of the zinc nanoparticle. XRD analyses revealed the average size of zinc nanoparticles as 33.31 nm for nanoparticles using zinc sulphate as precursors. Finally XRD result shows that postbiotics-exopolysaccharides zinc oxide nanoparticles are crystalline nature in the average size of 33.31 nm.

Hence we can confirm that XRD peaks of postbiotics-exopolysaccharides zinc oxide nanoparticles are crystalline in nature with an average size of 33.31 nm.

The particle size of the synthesized zinc oxide nanoparticles was in close agreement with the study [10] with average crystalline sizes 21.49 and 25.26nm. These values obtained are in close proximities of our study to conclude the particles are zinc oxide nanoparticles. Thus, the XRD analysis has shown that zinc oxide nanoparticles with well-defined dimensions could be synthesized by reduction of metal ions due to postbiotics-exopolysaccharides.

#### 4. DISCUSSION

Exopolysaccharides producing cultures are widely used in dairy foods to provide viscosity, stability and water-binding functions to dairy products which are contributed positively to the mouth-feel, texture and taste perception of fermented dairy products. One of the most important commercial applications of exopolysaccharides is in yogurt manufacture in which Lactic Acid Bacteria (e.g. *S. thermophilus*) is authoritatively used in dairy foods [11]. *Lactobacillus helveticus* has the characteristic exopoly-saccharides which increases water absorption, dough development time and dough stability in biscuit production process and thus the shelf life of biscuit is lengthened [12].

Exopolysaccharides like pullulan are used as a partial replacement for starch in pastas or baked goods. Pullulan solutions are of relatively low viscosity, resembling gum Arabic, thus used as low viscosity filler in beverages and sauces. Pullulan are used as a denture adhesive, a binder and stabilizer in food pastes and to adhere nuts to cookies. Pullulan films are formed by drying a pullulan solution onto an appropriate smooth surface. This property is used to protect fruits such as apples to improve their shelf life films have the thickness of about 5-60 um, these films are clear, highly oxygen-impermeable and have excellent mechanical properties, thus keeping the fruits fresh for long duration, prevent fruits from wear and tear in transport period. As these films readily dissolve in water, they melt in the mouth as edible food coatings and do not possess any harmful effects as that of wax coatings normally used for fruits to keep them fresh. Specialty films may include colours or flavours. Decorative pullulan chips are produced for food uses. Alternatively, pullulan can be applied directly to foods as a protective glaze [13].

Exopolysaccharides may function as viscosifying agents, stabilizers, emulsifiers, gelling agents, or water-binding agents in food [14]. Large number of polysaccharides used in foods is of plant origin. EPS produced by microorganism have unique rheological properties

because of their capability of forming very viscous solutions at low concentrations due to their pseudo plastic nature [15].

Exopolysaccharides from lactic acid bacteria have found their valuable application in the improvement of the rheological properties of fermented dairy products. Microbial exopolysaccharides function as bio-thickeners, stabilizers, gelling agents, viscosifying agents or water binding agents. Exopolysaccharides production significantly contributes to texture, mouth feel, teats and stability of the final dairy product. Exopolysaccharides are low fat, sugar content and low levels of food additives, as well as cost factors, make microbial exopolysaccharides a profitable alternative of artificial food additives.

Exopolysaccharides are structural components of the extracellular matrix in which cells are embedded during biofilm development [16]. In a wide sense an exopolysaccharide can be defined as any long chain polysaccharide linear or branched that is soluble in water, has the capacity, in solution, of increasing the viscosity and/or form gels. Microbial exopolysaccharides display encouraging therapeutic potential in terms of immuno-modulation, anti-oxidation, hypercholesterolemia and promotion of a functional digestive tract through probiotic activity. It is clear that certain exopolysaccharide structures play central roles in the bioactivity of the microbial producer and thus, may be important in reclaiming an EFSA "probiotic" immune modulatory health claim. Indeed, the impact of exopolysaccharides on human health appears to be multifactorial and structure-function related [17].

One of the most remarkable and useful features of a polysaccharide's swelling ability manifests itself when it is triggered by a change in the environment surrounding the delivery system. Many of the potentially useful pH sensitive polymers swell at high pH values and collapse at low pH values, trigger the drug delivery upon an increase in the pH of the environment. Such materials are ideal for systems such as oral delivery, in which the drug is not released at low pH values in the stomach, but rather at high pH values in the upper small intestine [18]. Natural polysaccharides are extensively used for the development of solid dosage forms. These polymers of mono-saccharaides (sugars) are inexpensive and available in a variety of structures with a variety of properties. They are highly stable, safe, non-toxic and hydrophilic and gel forming in nature. Pectin, starch, guar gum, amylose and karaya gum are a few

polysaccharides commonly used in dosage forms. Non-starch, linear polysaccharides remain intact in the physiological environment of the stomach and the small intestine, but are degraded by the bacterial inhabitants of the human colon which make them potentially useful in targeted delivery systems to the colon [19].

Silver and zinc oxide nanoparticles have some similarities such as their inorganic nature, a variety of synthesis methods and toxicity to the environment, among others. However, differences in bioavailability, applications and regulations offer some advantages to zinc oxide nanoparticles incorporated in polymeric matrices when compared to silver nanoparticles including providing solutions for safer and more affordable antimicrobial food packaging [5]. The main applications of zinc oxide nanoparticles for food packaging materials include providing antimicrobial activity, since the presence of zinc oxide nanoparticles in the polymeric matrix allows the packaging to interact with the food and have a dynamic role in their preservation. In addition, zinc oxide nanoparticles allow for the improvement of packaging properties such as mechanical strength, barrier properties and stability. Zinc oxide nanoparticles have been incorporated in different materials including glass, Low Density Polyethylene (LDPE), Polypropylene (PP), Polyurethane (PU), paper and chitosan using different incorporation methods [20]. Zinc oxide is a compound with many applications in everyday life. In addition, zinc oxide in Nano size is a promising antimicrobial agent due to its activity against a wide range of microorganisms and high resistance to severe processing conditions. Zinc oxide nanoparticles have antimicrobial properties against foodborne pathogens. Antimicrobial food packaging developed with nanotechnology represents an impact on consumers and also effect on food safety [5].

## 5. CONCLUSION

The study shows the presence of water OH stretches, alcohol OH stretching, carboxylic acid, N-H stretching, C-H stretching, =C-H stretching, -C-H stretching, -C-H aldehydic, C-N stretching, C-C stretching, C=O aldehyde, C=O anhydride, C=O ester, C=O ketone, C=O amide, C=C Alkene, C=C aromatic, C-O-C stretch, C-OH stretching, NO<sub>2</sub> stretching, C-F, C-Cl, C-Br, Zn-O stretching, carbohydrate band (C-O), polysaccharides, galactose and mannose and C-I determined using FTIR analysis.

The main significance of the study is develop antimicrobial coating using postbiotics-exopolysaccharides for extending the shelf life of the food products and also for improving the health status of the individuals. The recommendations that emerge out from the present study are development and evaluation of edible films using postbiotics-exopolysaccharides zinc oxide nanoparticles, development and evaluation of biodegradable films using postbiotics-exopolysaccharides zinc oxide nanoparticles, encapsulation of active components of postbiotics-exopolysaccharides zinc oxide nanoparticles into edible food packaging materials and *in vitro* studies for bioavailability of postbiotics-exopolysaccharides zinc oxide nanoparticles.

## Conflicts of Interest

The authors declare no conflict of interest.

## 6. REFERENCES

1. Malashree L, Angadi KV, Yadav S, Prabha V. *International Journal Current Microbiology Applied Sciences*, 2019; **8(1)**:2049-2053.
2. Leo F, Hashida S, Kumagai D, Uchida K, Motoshima H, Arai L, Asakuma S, Fukuda K, Urashima T. *Journal of Applied Glycoscience*, 2007; **54(4)**:223-229.
3. Mikelsaar M, Zilmer M. *Microbial Ecology in Health and Disease*, 2009; **21(1)**:1-27.
4. Elshama SS, Metwally E, Abdallah, Rehab I, Karim A. *The Open Nanomedicine Journal*, 2018; **5(1)**: 16-22.
5. Espitia PJP, Soares NDF, Coimbra JSJR, Andrade NJD, Cruz RS, Medeiros EAA. *Food Bioprocess Technology*, 2012; **5(1)**:1447-1464
6. Shehab A M, Saad AM, Moghannem M, Farag MS, Azab MS. *International Journal of Advanced Research in Biological Sciences*, 2017; **4(3)**:16-30.
7. Nwosu IG, Abu GO, Agwa KO. *Journal of Advances in Microbiology*, 2019; **19(2)**:1-13.
8. Trabelsi I, slima SB, Chaabane H, Riadh BS. *International Journal of Biological Macromolecules*, 2015; **74(1)**:541-546.
9. Hamedani NH, Farzaneh F. *Journal of Sciences*, 2006; **17(3)**:231-234.
10. Fakhari S, Hassan MJ, Fard K. *Green Chemistry Letters and Reviews*, 2019; **12(1)**:19-24.
11. Broadbent JR, McMahan DJ, Welker DL, Oberg CJ, Moineau S. *Journal of Dairy Sciences*, 2003; **86(2)**:407-423.
12. Hussein AS, Ibrahim GS, Asker MMS, Mahmoud MG. *Journal of Food Science*, 2010; **28(10)**:225- 232.

13. Leathers TD. (2003). *Applied Microbiology Biotechnology*, 2003; **62(5)**:468-473.
14. Van den Berg DJC, Robijn GW, Janssen AC, Giuseppin MLF, Vreeker R, Kamerling JP, et al. *Applied and Environment Microbiology*, 1995; **61(8)**:2840-2844.
15. Becker A, Katzen F, Pühler A, Ielpi L. *Applied Microbiology Biotechnology*, 1998; **50(1)**:145-152.
16. Marvasi M, Pieter T, Visscher, Martinez LS. *Journal of Federation of European Microbiological Societies*, 2010; **313(1)**:1-9.
17. Ryan PM, Ross RP, Fitzgerald GF, Caplice NM, Stanton C. *Journal of Food and Function*, 2015; **1(3)**:679-693.
18. Manjanna KM, Kumar TMP, Shivakumar B. *International Journal of Chemistry Tech. Research*, 2010; **2(1)**:509-525.
19. Singh RP, Singh SG, Naik H, Jain D, Bisla S. *International Journal of Comprehensive Pharmacy*, 2011; **4(2)**:1-4.
20. Ghule K, Ghule AV, Chen BJ, Ling YC. *Journal of Green Chemistry*, 2016; **8(12)**:1034-1041.